Order online now!

www.rockland.com
tech@rockland.com
+1 484.791.3823

Datasheet for 18-8817-33

Mouse TrueBlot® ULTRA: Anti-Mouse Ig HRP

Overview

Description:	Mouse TrueBlot® ULTRA: Anti-Mouse Ig HRP - 18-8817-33
Item No.:	18-8817-33
Size:	200 µL
Applications:	ELISA, IP, WB, Biochemical Assay, ChIP, IF
Reactivity:	Mouse
Host Species:	Rat

Product Details

Background:	Mouse IgG TrueBlot® ULTRA is a unique Anti-Mouse IgG monoclonal secondary antibody. Mouse IgG TrueBlot® ULTRA enables detection of immunoblotted target protein bands, without hindrance by interfering immunoprecipitating immunoglobulin heavy and light chains. It is easy to generate publication-quality IP/Western blot data with Mouse IgG TrueBlot® ULTRA, simply substitute the conventional Anti-Mouse IgG blotting reagent with Mouse IgG TrueBlot® ULTRA and follow the prescribed protocol for sample preparation and immunoblotting. Mouse IgG TrueBlot® ULTRA is ideal for use in protocols involving immunoblotting of immunoprecipitated proteins. Mouse IgG TrueBlot® ULTRA preferentially detects the non-reduced form of mouse IgG (IgG1, IgG2a, IgG2b, IgG3) over the reduced, SDS-denatured form of IgG. When the immunoprecipitate is fully reduced immediately prior to SDS-gel electrophoresis, reactivity of Mouse IgG TrueBlot® ULTRA with the 55 kDa heavy chains and the 23 kDa light chains of the immunoprecipitating antibody is minimized thereby eliminating interference by the heavy and light chains of the immunoprecipitating antibody in IP/immunoblot applications. Applications include studies examining post-translational modification (e.g., phosphorylation or acetylation) or protein-protein interactions.
Synonyms:	Anti-Mouse IgG HRP, TrueBlot, HRP TrueBlot ULTRA, Peroxidase TrueBlot, TrueBlot for IP/WB, TrueBlot for immunoprecipitation, TrueBlot for western blotting
Host Species:	Rat
Conjugate:	Peroxidase (HRP) ULTRA
Clonality:	Monoclonal
Clone ID:	eB144
Format:	IgG

F/P Ratio:	1.446

Target Details

Reactivity:	Mouse
Purity/Specificity:	Mouse TrueBlot® ULTRA Antibody Peroxidase Conjugate was prepared from tissue culture supernatant by Protein G affinity chromatography. Assay by immunoelectrophoresis resulted in a single precipitin arc against Anti-Mouse Serum. Reactivity is observed against native Mouse IgG by both Western blot and ELISA.
Relevant Links:	• TrueBlot HRP Product Protocols • TrueBlot IP Set Protocol • SDS

Application Details

Tested Applications:	ELISA, IP, WB
Suggested Applications:	Biochemical Assay, ChIP, IF (Based on references)
Application Note:	Mouse TrueBlot® ULTRA has been tested in ELISA, IP, and Western blot and may also be used for detection in immunoblotting assays that do not employ immunoprecipitation. Mouse IgG TrueBlot® ULTRA is provided as 1000X solution. To achieve best results when detecting mouse IgG1 subtypes, we recommend performing a dot blot or titration to determine the optimal dilution factor for your desired application. All recommended dilutions for listed applications are intended as an initial recommendation, specific conditions for each protein and antibody combination should be specifically optimized by the end user. In order to conserve reagent, we recommend incubating the blots from minigels in sealed bags (removing as much air as possible) with minimal volume (2-3 mLs). If used conservatively at 2.5mls/blot will yield enough reagent for 8 blots. Note that there are three key procedural considerations: 1. Protein A or G beads may be used with the mouse, goat and sheep TrueBlot secondaries, but not with the rabbit TrueBlot secondary. Use of protein A or G beads with the rabbit TrueBlot will result in contaminating bands. 2. Immunoprecipitate should be completely reduced. 3. BLOTTO/Milk should be used as the blocking protein for the immunoblot.
Assay Dilutions:	All assays should be optimized by the user. Recommended dilutions (if any) may be listed below.
IF:	User Optimized
IP:	User Optimized
WB:	1:1000

Formulation

Physical State:	Liquid (sterile filtered)
Concentration:	1 mg/mL by UV absorbance at 280 nm
Buffer:	0.02 M Potassium Phosphate, 0.15 M Sodium Chloride, pH 7.2
Preservative:	0.01% (w/v) Gentamicin Sulfate
Stabilizer:	0.1 mg/ml Bovine Serum Albumin (BSA) - IgG and Protease free, 50% (v/v) Glycerol

Shipping & Handling

Shipping Condition:	Wet Ice
Storage Condition:	Store at -20°C. This product is guaranteed for 6 months upon receipt, when handled and stored as instructed.
Expiration:	Expiration date is six (6) months from date of receipt.

Images

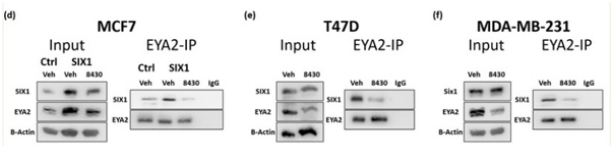

Western Blot

Compound 8430 disrupts SIX1-EYA2 interaction in breast cancer cells.

d-f. EYA2 Immunoprecipitation (IP) followed by Western Blot (WB) analyses. Representative images (n=3) of WBs demonstrate levels of SIX1 and EYA2 in input and in the EYA2-IP fractions in vehicle vs 8430 treated MCF7-Ctrl/SIX1 (d), T47D (e), and MDA-MB-231 (f) cells. Cells were lysed using ELB buffer (250mM NaCl, 50mM Hepes pH 7.0, 5mM EDTA and 0.1% NP40), and protein samples were pre-cleared using TrueBlot anti-Rabbit IgG Magnetic beads (p/n 00-1800-50). Samples were then incubated with 2µg of antibody targeting EYA2: anti-EYA2 IgG and 50µl of TrueBlot magnetic beads overnight at 4 °C, while gently rocking. The following day, beads were washed using TBS, and proteins were dissociated from the beads by boiling the sample with loading buffer prior to the Western Blotting analyses. Of note, secondary antibodies used during Western Blot analyses only recognize non-denatured IgG (Rabbit TrueBlot ULTRA Anti-Rabbit IgG HRP (p/n 18-8816-31) and Mouse TrueBlot ULTRA Anti-Mouse IgG HRP (p/n 18-8817-33)). Fig3. D, E, F. PMID: 32341035.

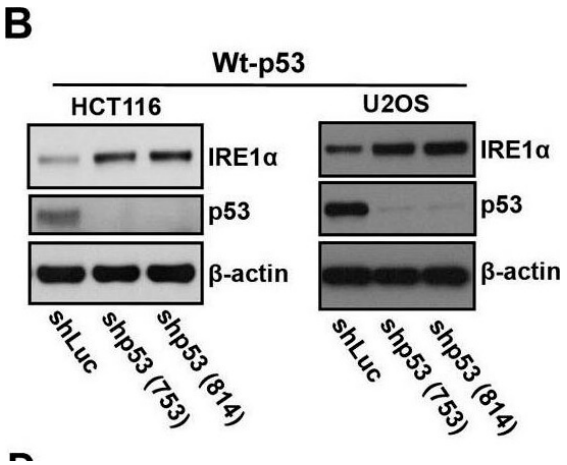

Western Blot

IRE1α expression is regulated by p53. A.) Western blot analysis of the expression of endogenous IRE1α in 23 human cancer cell lines. Cell lines were grouped according to expression of wild-type or mutant p53 as indicated. (A well between wt-p53 and mutant-p53 cell lines was cut, from the gel as indicated by a black line, due to the controversial p53 status of the cell line). Right panel: The intensities of the IRE1α bands (left panel) are expressed relative to those of β-actin. Values shown are the mean ± standard deviation (s.d.). The P value was calculated using two-way ANOVA. B.) Downregulation of p53 expression induces increased expression of IRE1α. HCT116 p53+/+ and U2OS cells were transfected with shLuc, shp53 (753), or shp53 (814), and selected using puromycin. Whole cell lysates of a pool of transfectants were analyzed using western blotting with the indicated antibodies. C.) Overexpression of wild-type p53 inhibits IRE1α expression in mutant-p53 cell lines. Cell lysates, prepared 48 h after transfection with wild-type p53, were analyzed for the expression of indicated proteins. D.) Mutant p53 proteins do not inhibit IRE1α expression. Cell lysates were prepared from cells transfected with p53-G245S, p53-R248W, p53-249S, and p53-R273H expression vectors or from cells that constitutively expressed wild-type p53 and were analyzed for the expression of the indicated proteins. Figure provided by CiteAb. Source: Oncotarget, PMID: 26254280.

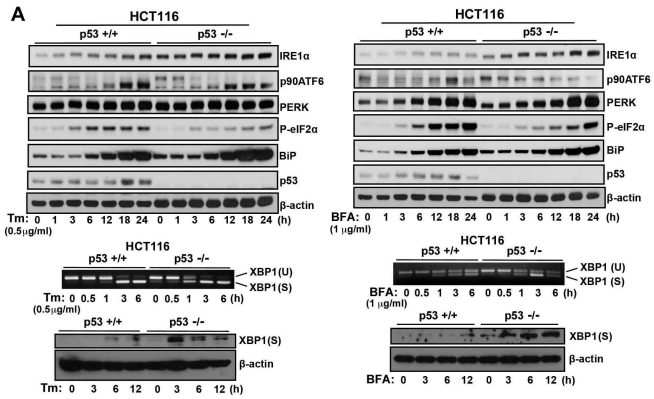

Western Blot

ER stress response in p53-deficient or knockdown cells. A.) HCT116 p53+/+ or HCT116 p53−/− cells, B. MEF p53+/+ or MEF p53−/− cells, and C. U2OS shLuc or U2OS shp53 cells were incubated with Tm (0.5 μg/mL) or BFA (1 μg/mL) for the times indicated. Cell lysates were analyzed using western blotting with the indicated antibodies. The blot was cut based on the size of proteins or stripped. Total RNAs were extracted and subjected to RT-PCR analysis using specific primer sets for XBP1(U) and XBP1(S). Cell lysates were analyzed using western blotting with indicated antibodies. Figure provided by CiteAb. Source: Oncotarget, PMID: 26254280.

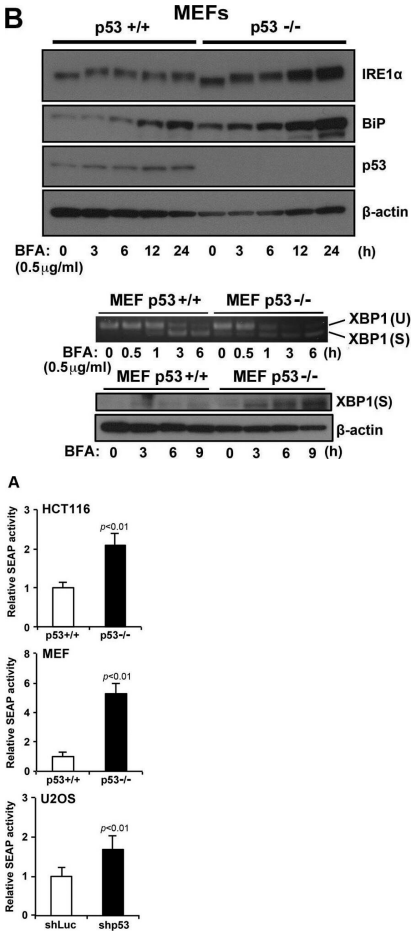

Western Blot

ER stress response in p53-deficient or knockdown cells. A.) HCT116 p53+/+ or HCT116 p53−/− cells, B.) MEF p53+/+ or MEF p53−/− cells, and C.) U2OS shLuc or U2OS shp53 cells were incubated with Tm (0.5 μg/mL) or BFA (1 μg/mL) for the times indicated. Cell lysates were analyzed using western blotting with the indicated antibodies. The blot was cut based on the size of proteins or stripped. Total RNAs were extracted and subjected to RT-PCR analysis using specific primer sets for XBP1(U) and XBP1(S). Cell lysates were analyzed using western blotting with indicated antibodies. Figure provided by CiteAb. Source: Oncotarget, PMID: 26254280.

Western Blot

p53 deficiency increases secretory the function of the ER through the IRE1α/XBP1 pathway. A.) HCT116 p53+/+ or HCT116 p53−/− cells, MEF p53+/+ or MEF p53−/− cells, and U2OS shLuc or U2OS shp53 cells expressing secreted embryonic alkaline phosphatase (SEAP) were transduced with a pSEAP2 control vector and washed 24 h after transduction. The medium was then changed, and the cells were cultured for another 6 h. Culture media were analyzed for SEAP activity, and luminescence was normalized to cell number. The transfection efficiencies of HCT116 p53+/+ and HCT116 p53−/− cells were approximately 80% each (data not shown). B.) Overexpression of wild-type p53 inhibited SEAP activity. SEAP activities of cells that constitutively expressed the indicated p53 molecules were analyzed using the same procedure described in (A). C.) HCT116 p53−/− cells that expressed SEAP were transfected with siControl, siATF6, siPERK, or siIRE1α, cultured for 24 h, and following a change of medium, the cells were cultured for another 6 h. Whole cell lysates were analyzed using western blotting with the indicated antibodies, and culture supernatants were analyzed for SEAP activity. Values shown are the mean ± s.d. of three different experiments simultaneously measured. The P value was calculated using two-way ANOVA. Figure provided by CiteAb. Source: Oncotarget, PMID: 26254280.

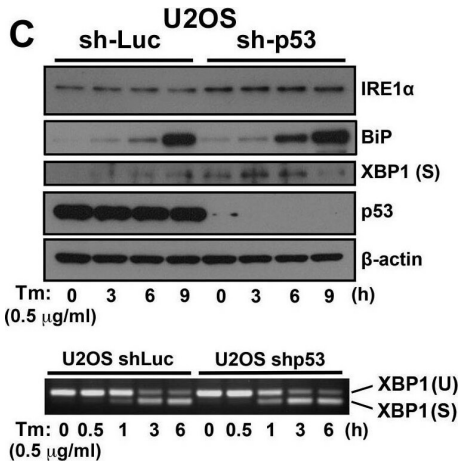

Western Blot

ER stress response in p53-deficient or knockdown cells. A.) HCT116 p53+/+ or HCT116 p53−/− cells, B. MEF p53+/+ or MEF p53−/− cells, and C. U2OS shLuc or U2OS shp53 cells were incubated with Tm (0.5 μg/mL) or BFA (1 μg/mL) for the times indicated. Cell lysates were analyzed using western blotting with the indicated antibodies. The blot was cut based on the size of proteins or stripped. Total RNAs were extracted and subjected to RT-PCR analysis using specific primer sets for XBP1(U) and XBP1(S). Cell lysates were analyzed using western blotting with indicated antibodies. Figure provided by CiteAb. Source: Oncotarget, PMID: 26254280.

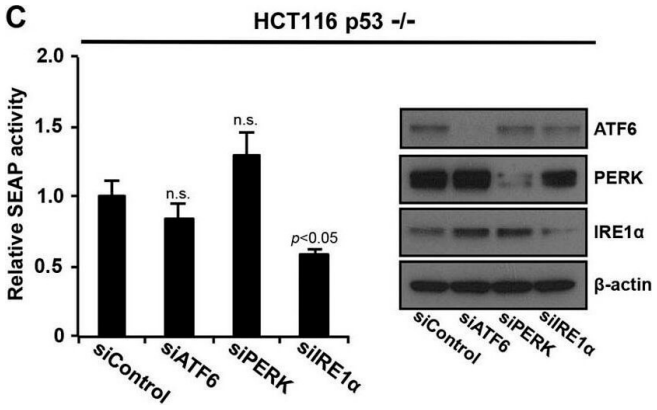

Western Blot

p53 deficiency increases secretory the function of the ER through the IRE1α/XBP1 pathway. A.) HCT116 p53+/+ or HCT116 p53−/− cells, MEF p53+/+ or MEF p53−/− cells, and U2OS shLuc or U2OS shp53 cells expressing secreted embryonic alkaline phosphatase (SEAP) were transduced with a pSEAP2 control vector and washed 24 h after transduction. The medium was then changed, and the cells were cultured for another 6 h. Culture media were analyzed for SEAP activity, and luminescence was normalized to cell number. The transfection efficiencies of HCT116 p53+/+ and HCT116 p53−/− cells were approximately 80% each (data not shown). B.) Overexpression of wild-type p53 inhibited SEAP activity. SEAP activities of cells that constitutively expressed the indicated p53 molecules were analyzed using the same procedure described in (A). C.) HCT116 p53−/− cells that expressed SEAP were transfected with siControl, siATF6, siPERK, or siIRE1α, cultured for 24 h, and following a change of medium, the cells were cultured for another 6 h. Whole cell lysates were analyzed using western blotting with the indicated antibodies, and culture supernatants were analyzed for SEAP activity. Values shown are the mean ± s.d. of three different experiments simultaneously measured. The P value was calculated using two-way ANOVA. Figure provided by CiteAb. Source: Oncotarget, PMID: 26254280.

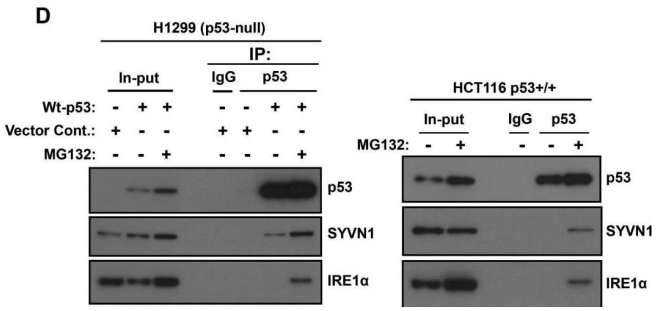

Western Blot

Synoviolin promotes IRE1α degradation in a wild-type p53-dependent manner. A.) SYVN1 suppresses IRE1α protein expression in wild-type p53 cells. HCT116 p53+/+ or HCT116 p53−/− cells were transfected with siControl (−) or siSYVN1 (+) and cultured for 24 h. Cell lysates were analyzed using western blotting with indicated the antibodies (left panel). The intensities of the SYVN1 bands were quantified. The levels of SYVN1 are reported relative to those of β-actin (right panel). The blot was cut based on the size of proteins or stripped and reprobed. B.) IRE1α and SYVN1 interaction is suppressed in p53-deficient cells. Proteins were cross-linked with DSP before protein extraction. Coimmunoprecipitation was performed with cell lysate using an IRE1α or an SYVN1 antibody. C.) SYVN1 interacts with wild-type p53. H1299 cells transiently expressed wild-type p53, p53-R248S, or p53-R273H. Coimmunoprecipitation experiments were performed using the anti-p53 antibody. D.) p53-SYVN1-IRE1α complex is observed by treatment with proteasome inhibitor. H1299 cells transiently expressing wild-type p53 (left panel) or HCT116 p53+/+ (right panel) cells were treated with 50 μM MG132 for 3 h. Coimmunoprecipitation experiments were performed using the anti-p53 antibody. Figure provided by CiteAb. Source: Oncotarget, PMID: 26254280.

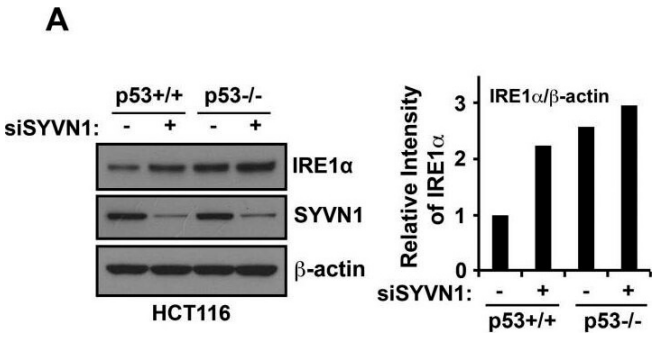

Western Blot

Synoviolin promotes IRE1α degradation in a wild-type p53-dependent manner. A.) SYVN1 suppresses IRE1α protein expression in wild-type p53 cells. HCT116 p53+/+ or HCT116 p53−/− cells were transfected with siControl (−) or siSYVN1 (+) and cultured for 24 h. Cell lysates were analyzed using western blotting with indicated the antibodies (left panel). The intensities of the SYVN1 bands were quantified. The levels of SYVN1 are reported relative to those of β-actin (right panel). The blot was cut based on the size of proteins or stripped and reprobed. B.) IRE1α and SYVN1 interaction is suppressed in p53-deficient cells. Proteins were cross-linked with DSP before protein extraction. Coimmunoprecipitation was performed with cell lysate using an IRE1α or an SYVN1 antibody. C.) SYVN1 interacts with wild-type p53. H1299 cells transiently expressed wild-type p53, p53-R248S, or p53-R273H. Coimmunoprecipitation experiments were performed using the anti-p53 antibody. D.) p53-SYVN1-IRE1α complex is observed by treatment with proteasome inhibitor. H1299 cells transiently expressing wild-type p53 (left panel) or HCT116 p53+/+ (right panel) cells were treated with 50 μM MG132 for 3 h. Coimmunoprecipitation experiments were performed using the anti-p53 antibody. Figure provided by CiteAb. Source: Oncotarget, PMID: 26254280.

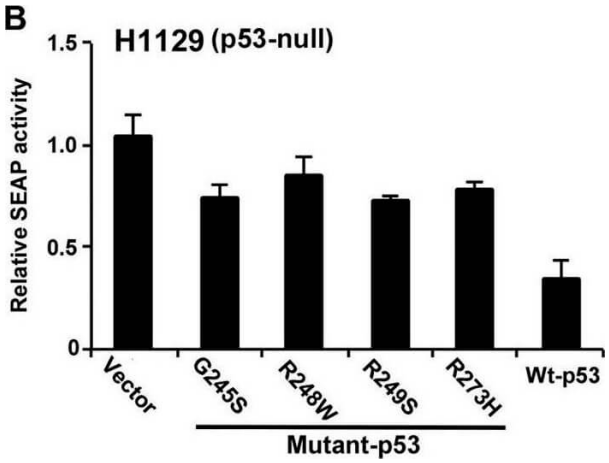

Western Blot

p53 deficiency increases secretory the function of the ER through the IRE1α/XBP1 pathway. A.) HCT116 p53+/+ or HCT116 p53−/− cells, MEF p53+/+ or MEF p53−/− cells, and U2OS shLuc or U2OS shp53 cells expressing secreted embryonic alkaline phosphatase (SEAP) were transduced with a pSEAP2 control vector and washed 24 h after transduction. The medium was then changed, and the cells were cultured for another 6 h. Culture media were analyzed for SEAP activity, and luminescence was normalized to cell number. The transfection efficiencies of HCT116 p53+/+ and HCT116 p53−/− cells were approximately 80% each (data not shown). B.) Overexpression of wild-type p53 inhibited SEAP activity. SEAP activities of cells that constitutively expressed the indicated p53 molecules were analyzed using the same procedure described in (A). C.) HCT116 p53−/− cells that expressed SEAP were transfected with siControl, siATF6, siPERK, or siIRE1α, cultured for 24 h, and following a change of medium, the cells were cultured for another 6 h. Whole cell lysates were analyzed using western blotting with the indicated antibodies, and culture supernatants were analyzed for SEAP activity. Values shown are the mean ± s.d. of three different experiments simultaneously measured. The P value was calculated using two-way ANOVA. Figure provided by CiteAb. Source: Oncotarget, PMID: 26254280.

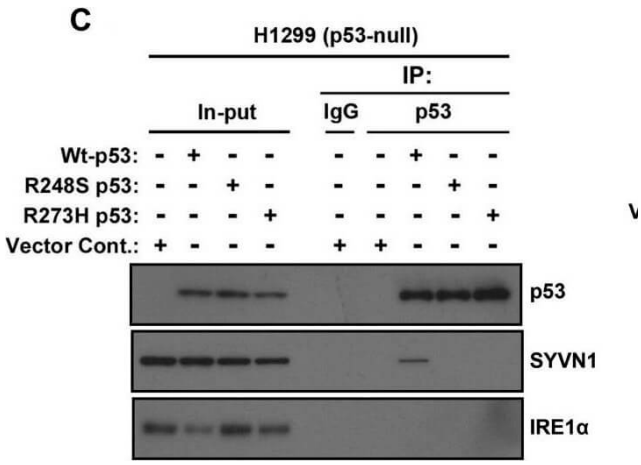

Western Blot

Synoviolin promotes IRE1α degradation in a wild-type p53-dependent manner. A.) SYVN1 suppresses IRE1α protein expression in wild-type p53 cells. HCT116 p53+/+ or HCT116 p53−/− cells were transfected with siControl (−) or siSYVN1 (+) and cultured for 24 h. Cell lysates were analyzed using western blotting with indicated the antibodies (left panel). The intensities of the SYVN1 bands were quantified. The levels of SYVN1 are reported relative to those of β-actin (right panel). The blot was cut based on the size of proteins or stripped and reprobed. B.) IRE1α and SYVN1 interaction is suppressed in p53-deficient cells. Proteins were cross-linked with DSP before protein extraction. Coimmunoprecipitation was performed with cell lysate using an IRE1α or an SYVN1 antibody. C.) SYVN1 interacts with wild-type p53. H1299 cells transiently expressed wild-type p53, p53-R248S, or p53-R273H. Coimmunoprecipitation experiments were performed using the anti-p53 antibody. D.) p53-SYVN1-IRE1α complex is observed by treatment with proteasome inhibitor. H1299 cells transiently expressing wild-type p53 (left panel) or HCT116 p53+/+ (right panel) cells were treated with 50 μM MG132 for 3 h. Coimmunoprecipitation experiments were performed using the anti-p53 antibody. Figure provided by CiteAb. Source: Oncotarget, PMID: 26254280.

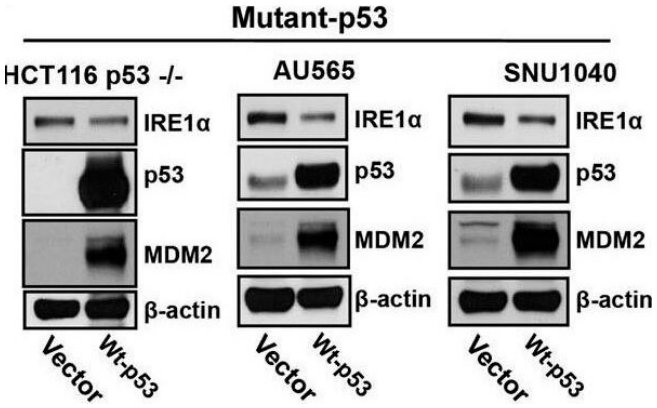

Western Blot

IRE1α expression is regulated by p53. A.) Western blot analysis of the expression of endogenous IRE1α in 23 human cancer cell lines. Cell lines were grouped according to expression of wild-type or mutant p53 as indicated. (A well between wt-p53 and mutant-p53 cell lines was cut, from the gel as indicated by a black line, due to the controversial p53 status of the cell line). Right panel: The intensities of the IRE1α bands (left panel) are expressed relative to those of β-actin. Values shown are the mean ± standard deviation (s.d.). The P value was calculated using two-way ANOVA. B.) Downregulation of p53 expression induces increased expression of IRE1α. HCT116 p53+/+ and U2OS cells were transfected with shLuc, shp53 (753), or shp53 (814), and selected using puromycin. Whole cell lysates of a pool of transfectants were analyzed using western blotting with the indicated antibodies. C.) Overexpression of wild-type p53 inhibits IRE1α expression in mutant-p53 cell lines. Cell lysates, prepared 48 h after transfection with wild-type p53, were analyzed for the expression of indicated proteins. D.) Mutant p53 proteins do not inhibit IRE1α expression. Cell lysates were prepared from cells transfected with p53-G245S, p53-R248W, p53-249S, and p53-R273H expression vectors or from cells that constitutively expressed wild-type p53 and were analyzed for the expression of the indicated proteins. Figure provided by CiteAb. Source: Oncotarget, PMID: 26254280.

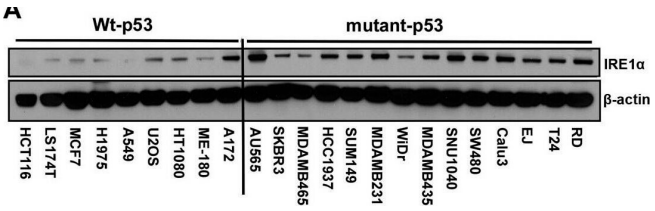

Western Blot

IRE1α expression is regulated by p53. A.) Western blot analysis of the expression of endogenous IRE1α in 23 human cancer cell lines. Cell lines were grouped according to expression of wild-type or mutant p53 as indicated. (A well between wt-p53 and mutant-p53 cell lines was cut, from the gel as indicated by a black line, due to the controversial p53 status of the cell line). Right panel: The intensities of the IRE1α bands (left panel) are expressed relative to those of β-actin. Values shown are the mean ± standard deviation (s.d.). The P value was calculated using two-way ANOVA. B.) Downregulation of p53 expression induces increased expression of IRE1α. HCT116 p53+/+ and U2OS cells were transfected with shLuc, shp53 (753), or shp53 (814), and selected using puromycin. Whole cell lysates of a pool of transfectants were analyzed using western blotting with the indicated antibodies. C.) Overexpression of wild-type p53 inhibits IRE1α expression in mutant-p53 cell lines. Cell lysates, prepared 48 h after transfection with wild-type p53, were analyzed for the expression of indicated proteins. D.) Mutant p53 proteins do not inhibit IRE1α expression. Cell lysates were prepared from cells transfected with p53-G245S, p53-R248W, p53-249S, and p53-R273H expression vectors or from cells that constitutively expressed wild-type p53 and were analyzed for the expression of the indicated proteins. Figure provided by CiteAb. Source: Oncotarget, PMID: 26254280.

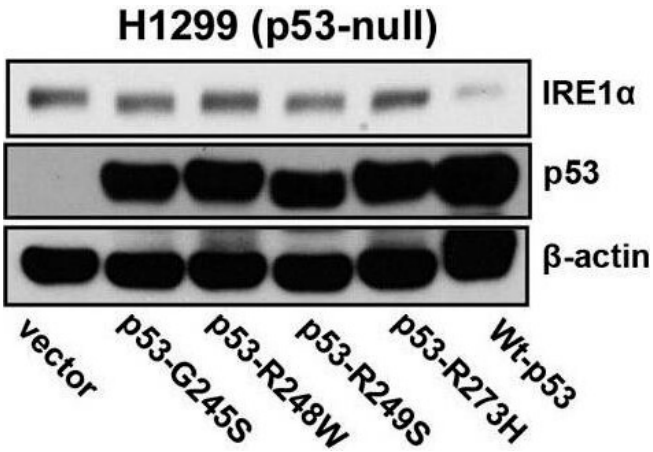

Western Blot

IRE1α expression is regulated by p53. A.) Western blot analysis of the expression of endogenous IRE1α in 23 human cancer cell lines. Cell lines were grouped according to expression of wild-type or mutant p53 as indicated. (A well between wt-p53 and mutant-p53 cell lines was cut, from the gel as indicated by a black line, due to the controversial p53 status of the cell line). Right panel: The intensities of the IRE1α bands (left panel) are expressed relative to those of β-actin. Values shown are the mean ± standard deviation (s.d.). The P value was calculated using two-way ANOVA. B.) Downregulation of p53 expression induces increased expression of IRE1α. HCT116 p53+/+ and U2OS cells were transfected with shLuc, shp53 (753), or shp53 (814), and selected using puromycin. Whole cell lysates of a pool of transfectants were analyzed using western blotting with the indicated antibodies. C.) Overexpression of wild-type p53 inhibits IRE1α expression in mutant-p53 cell lines. Cell lysates, prepared 48 h after transfection with wild-type p53, were analyzed for the expression of indicated proteins. D.) Mutant p53 proteins do not inhibit IRE1α expression. Cell lysates were prepared from cells transfected with p53-G245S, p53-R248W, p53-249S, and p53-R273H expression vectors or from cells that constitutively expressed wild-type p53 and were analyzed for the expression of the indicated proteins. Figure provided by CiteAb. Source: Oncotarget, PMID: 26254280.

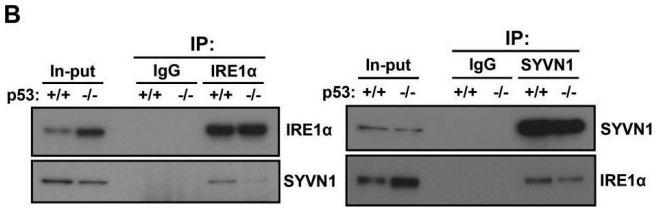

Western Blot

Synoviolin promotes IRE1α degradation in a wild-type p53-dependent manner. A.) SYVN1 suppresses IRE1α protein expression in wild-type p53 cells. HCT116 p53+/+ or HCT116 p53−/− cells were transfected with siControl (−) or siSYVN1 (+) and cultured for 24 h. Cell lysates were analyzed using western blotting with indicated the antibodies (left panel). The intensities of the SYVN1 bands were quantified. The levels of SYVN1 are reported relative to those of β-actin (right panel). The blot was cut based on the size of proteins or stripped and reprobed. B.) IRE1α and SYVN1 interaction is suppressed in p53-deficient cells. Proteins were cross-linked with DSP before protein extraction. Coimmunoprecipitation was performed with cell lysate using an IRE1α or an SYVN1 antibody. C.) SYVN1 interacts with wild-type p53. H1299 cells transiently expressed wild-type p53, p53-R248S, or p53-R273H. Coimmunoprecipitation experiments were performed using the anti-p53 antibody. D.) p53-SYVN1-IRE1α complex is observed by treatment with proteasome inhibitor. H1299 cells transiently expressing wild-type p53 (left panel) or HCT116 p53+/+ (right panel) cells were treated with 50 μM MG132 for 3 h. Coimmunoprecipitation experiments were performed using the anti-p53 antibody. Figure provided by CiteAb. Source: Oncotarget, PMID: 26254280.

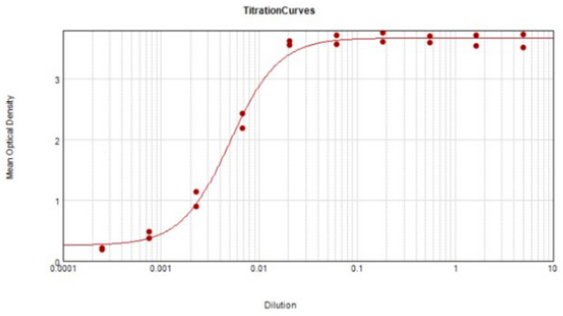

ELISA

ELISA Results of Mouse TrueBlot® ULTRA: Anti-Mouse Ig HRP. Each well was coated in duplicate with 1.0 μg of Mouse TrueBlot® ULTRA: Anti-Mouse Ig HRP (red line). The starting dilution of antibody was 5μg/ml and the X-axis represents the Log10 of a 3-fold dilution. The titer is 199,000. This titration is a 4-parameter curve fit where the IC50 is defined as the titer of the antibody. Assay performed using TMB-1000 substrate.

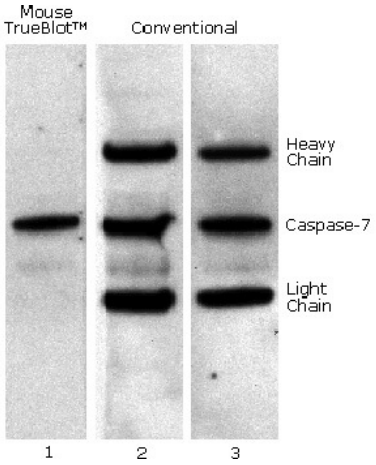

Western Blot
Mouse TrueBlot® IP / Western Blot: Caspase 7 was immunoprecipitated from 0.5 ml of 1x10e7 Jurkat cells/ml with 5 ug mouse anti-human Caspase 7. Precipitate from 1x10e6 cells was subjected to electrophoresis, transferred to an PVDF membrane, and Western blotted with anti-Caspase 7 using Mouse TrueBlot® ULTRA: Anti-Mouse Ig HRP (Lane 1) or conventional HRP-conjugated anti-mouse antibody (Lane 2) - note the detection of the heavy and light chains of the immunoprecipitating antibody in Lane 2 but not in Lane 1. When Lane 1 is re-immunoblotted using conventional HRP-conjugated anti-mouse polyclonal antibody (Lane 3), the heavy and light chains are now detected, confirming that although the immunoprecipitating heavy and light chains are present, Mouse TrueBlot® ULTRA: Anti-Mouse Ig HRP detects only native antibody and not denatured heavy and light chains.

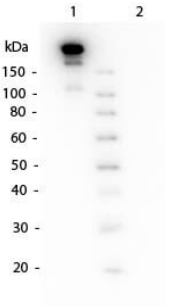

Western Blot
Western Blot of Mouse TrueBlot® ULTRA: Anti-Mouse Ig HRP. Lane 1: Mouse IgG, non-denatured. Center Lane: 5 µL Opal Pre-stained Ladder (p/n MB210-0500). Lane 2: Mouse IgG, denatured. Load: 50 ng. Primary antibody: none. Secondary antibody: Mouse TrueBlot® ULTRA: Anti-Mouse Ig HRP at 1:1,000 for 60 min at RT. Block: MB-070 for 30 min at RT. Predicted/Observed size: >160 kDa non-denatured for Mouse IgG.

References

- Fujiyama H et al. Diamond-Blackfan anemia gene product RPS19 counteracts SET to maintain p53 transcriptional activity and tumor suppressor function. *Cell Rep.* (2026)
- Xiang Q et al. Ubiquitin ligase ITCH regulates life cycle of SARS-CoV-2 virus. *Elife.* (2026)
- Mao R et al. RNA helicase DDX6 governs ASC speck formation in P-bodies and the transition to stress granules via phase separation during inflammasome activation. *Cell Discov.* (2026)
- Jusuf JM et al. Genome-wide absolute quantification of chromatin looping. *Nat Struct Mol Biol.* (2026)
- Khursigara MR et al. A cargo receptor entrapment complex is a therapeutic node for genetically and clinically distinct proteinopathies. *bioRxiv [Preprint]* (2026)

- Jin D et al. BRAF recruitment to spinal sensory synapses promotes neuropathic pain by potentiating transsynaptic NMDA receptor activity. *Sci Signal.* (2026)
- Uhl L et al. MYC binding to nascent RNA suppresses innate immune signaling by R-loop-derived RNA-DNA hybrids. *Cell.* (2026)
- Nass Jr. T et al. Cytosolic nucleic acid sensing triggers type I interferon activation via the Hippo kinase LATS1. *J Biol Chem.* (2026)
- Satapathy SR et al. Nuclear PD-L1 regulates YAP-driven transcription via the PGE2-EP4-YAP-importin α3 axis in solid tumors. *Cell Rep.* (2026)
- Jeong YS et al. Proliferation and Apoptosis Adaptor Protein 15 (PEA15), a Potential Oncogenic Regulator of VHL and HIF1A Identified through Proteomic Analysis in Hepatocellular Carcinoma. *Cancer Commun (Lond).* (2026)
- Shi JG et al. Capicua mediates interleukin-2 withdrawal-induced death of activated CD8+ T cells. *Cell Insight.* (2026)
- Hsu YJ et al. Discovery of BPR2-D2 compound in inhibiting Chikungunya viral RNA synthesis by replicon systems. *Biomed J.* (2026)
- Wang HH et al. Functional rescue of a disease-linked ERAD pathway mutation via alternative splicing. *EMBO J.* (2026)
- Assi M et al. Extracellular matrix sensing regulates intratumoral heterogeneity of autophagic flux. *Cell.* (2026)
- Martinez AE et al. Vimentin remodeling in response to oxidants and electrophiles is modulated by pH. *Sci Adv.* (2026)
- Murakami R et al. Foxp3 and BATF cooperatively direct cis-regulatory programs and gene expression for effector Treg cell differentiation. *Immunity.* (2026)
- Pang H et al. ZFP36L2 is an interferon β -induced inhibitor that restricts the nuclear export of HIV-1 transcripts. *Nat Commun.* (2026)
- Tang X et al. Nuclear N-glycosylation maintains H3K9me3 heterochromatin and genomic stability. *Nat Cell Biol.* (2026)
- Wang Q et al. The mechanistic role of the thromboxane A2 receptor (TBXA2R) in non-small cell lung cancer (NSCLC). *Cancer Cell Int.* (2026)
- Vit G et al. Schlafen regulates gastrulation in Xenopus laevis early embryonic development and exhibits immune tissue-specific expression in adult frogs. *Int J Dev Biol.* (2026)
- Kuang Z et al. The U1 snRNP protein U1C and Helix H of U1 snRNA are critical for small molecule splicing modulator function. *Nat Commun.* (2026)
- Tangermann C et al. Saturation mutagenesis identifies activating and resistance-inducing FGFR kinase domain mutations. *Nat Genet.* (2026)
- Sugimoto J et al. Mouse suppressyn-like 1 suppresses membrane fusion through envelope glycoprotein recognition. *Scientific Reports.* (2026)
- Min Y et al. The USP19-DnaJC7 Axis Stabilizes p53 in Cisplatin-Treated Epithelial Ovarian Cancer. *Cells.* (2026)
- Zhang X et al. An ancient mitochondrial program tunes translation to haem availability. *Nature.* (2026)
- Park M et al. Therapeutic Efficacy of PB101 and Chemotherapy Combination in Preclinical Gastric Cancer Models. *Anticancer Res.* (2026)

- Hirakata S et al. Transient residence of the repulsive client Shutdown in Yb bodies plays a critical role in Piwi-piRISC biogenesis and maintaining fertility. *Mol Cell.* (2026)
- Snell PH et al. Coordinated regulation of mRNA translation and stability by ZC3H7A and ZC3H7B RNA-binding proteins. *Cell Rep.* (2026)
- Wang Q et al. Deletion of p53-Related Protein Kinase Suppresses Solar UV-Induced Photocarcinogenesis by Inhibiting PD-L1 Expression and Enhancing CD8 T-Cell Infiltration. *J Invest Dermatol.* (2026)
- Lanz AJ et al. HDAC6-dependent deacetylation of SAE2 enhances SUMO1 conjugation for mitotic integrity. *EMBO J.* (2025)
- Wu P et al. Tissue-specific regulation of PNPLA3 promotes lipid remodeling in response to dietary and temperature stress. *bioRxiv [preprint]* (2025)
- Ageta H et al. Statins attenuate PD-L1 sorting to small extracellular vesicles dependent on ubiquitin-like 3 modification. *Sci Rep.* (2025)
- Shin JH et al. USP11 promotes colorectal cancer progression by stabilizing EGFR and TRAF6: a potential therapeutic target in EGFR- and TLR-driven tumorigenesis. *Cell Death Dis.* (2025)
- View More ...

Disclaimer

This product is for research use only and is not intended for therapeutic or diagnostic applications. Please contact a technical service representative for more information. All products of animal origin manufactured by Rockland Immunochemicals are derived from starting materials of North American origin. Collection was performed in United States Department of Agriculture (USDA) inspected facilities and all materials have been inspected and certified to be free of disease and suitable for exportation. All properties listed are typical characteristics and are not specifications. All suggestions and data are offered in good faith but without guarantee as conditions and methods of use of our products are beyond our control. All claims must be made within 30 days following the date of delivery. The prospective user must determine the suitability of our materials before adopting them on a commercial scale. Suggested uses of our products are not recommendations to use our products in violation of any patent or as a license under any patent of Rockland Immunochemicals, Inc. If you require a commercial license to use this material and do not have one, then return this material, unopened to: Rockland Inc., P.O. BOX 5199, Limerick, Pennsylvania, USA.